Available online at www.sciencedirect.com
SCIENCE DIRECT®
Journal of Nuclear Materials 329–333 (2004) 988–992
journal of nuclear materials
www.elsevier.com/locate/jnucmat

Electron spin resonance measurement of irradiation defects in vitreous silica irradiated with neutrons and ion beams

Kimikazu Moritani, Yoichi Teraoka, Ikuji Takagi, Hirotake Moriyama *

Department of Nuclear Engineering, Graduate School of Engineering, Kyoto University, Yoshida, Sakyo-ku, Kyoto 606-8501, Japan

Abstract

The electron spin resonance (ESR) measurement of irradiation defects in ion beam irradiated vitreous silica was performed. The spin densities of E′ centers, non-bridging oxygen hole centers (NBOHCs), and peroxy radicals (PORs) were measured as a function of the ion beam intensity, fluence, and post-irradiation isochronal annealing temperature. The results of the ion beam irradiation were compared with those of neutron irradiation, and both results were consistently explained by considering the dpa values of irradiation. Based on the proposed mechanism and mass balance, the concentration of the other defects such as oxygen deficiency centers (ODCs) were evaluated.

1. Introduction

In the case of vitreous silica, the three fundamental centers of the E′ center (≡Si·), the peroxy radical (POR: ≡Si—O—O·) and the non-bridging oxygen hole center (NBOHC: ≡ Si—O·) are known to form the basis of the present understanding of defects in this material [1]. These are all paramagnetic and have been well characterized by the electron spin resonance (ESR) techniques, compared with the diamagnetic oxygen-deficiency centers (ODCs:≡Si:Si≡). In addition, the self-trapped holes (STHs:≡Si—O—Si≡) are also known to participate in the radiolysis process in the lower temperature range, and it has been recently suggested that the STHs play an important role even at ambient temperature under irradiation [2].

In our recent study [3], ESR measurements were performed with neutron irradiated vitreous silica. Some new states were observed in the ESR spectra together with the usual paramagnetic states of the E′ centers, NBOHCs and PORs. The principal-axis *g*-values of the new states were obtained from the analysis, and were found to be typical of O_2^- ions in solids. Considering these defects, the observed effects of the OH content, neutron fluence, and post-irradiation isochronal anneal behaviors were well explained. Since their production yield saturates with the increasing neutron fluence, the observed new states are of rather minor importance and their production is hardly observed in the case of highly irradiated samples. It is interesting to evaluate this expectation with highly irradiated samples.

In the present study, for comparison, ESR measurement of irradiation defects in ion beam irradiated vitreous silica was performed to study the effects of the ion beam intensity, fluence, and post-irradiation isochronal anneal to 923 K. The results of the ion beam irradiation are compared with those of neutron irradiation to discuss some details of the reaction mechanism of the irradiation defects.

2. Experimental

Specimens of vitreous silica (T-2030, 1ppm OH) were obtained from Toshiba Ceramics Co., which were of 10 mm in diameter and about 0.5 mm in thickness. Specimens were irradiated with a He^+ ion beam, accelerated to 2 MeV with a Van de Graaff accelerator. The size of the ion beam was about 3 mm in diameter and its

* Corresponding author. Tel./fax: +81-75 753 5824.
E-mail address: moriyama@nucleng.kyoto-u.ac.jp (H. Moriyama).

0022-3115/$ - see front matter © 2004 Elsevier B.V. All rights reserved.
doi:10.1016/j.jnucmat.2004.04.311

intensity was monitored. The ion beam intensity ranged from 4.5×10^{-4} to 4.5×10^{-3} A m^{-2}, and the dose ranged from 2.0×10^{18} to 6.8×10^{19} ions m^{-2}.

After the irradiation, first-derivative ESR spectra were recorded either at room temperature (for the E′s) or at 77 K (for others) on a JEOL JES-TE200 instrument operating at X-band frequencies ($\nu \sim 9.26$ GHz) with 100-kHz magnetic field modulation. Measurements of the g-values were accomplished by using conventional standard samples of DPPH (diphenylpicrylhydrazyl) and MgO. Ten-minute isochronal anneals in 50 K increments were carried out by moving the samples contained in fused quartz sample tubes to an external furnace. Spin concentrations were determined by resolution of derivative spectra into a number of components, double numerical integration of every component spectra and comparison of the obtained areas with that of a DPPH sample of 1.53×10^{21} spins g^{-1}. The accuracy of the numerical integrations was typically of the order of ±5% for the stronger signals in the irradiated samples. In the case of the weaker signals, these errors were over ±10% due to low signal-to-noise ratios.

3. Results and discussion

3.1. Resolution of ESR spectra

Fig. 1 shows a typical ESR spectrum of ion beam irradiated vitreous silica of T-2030. As shown in this figure, the resolution of the observed spectra was well completed by only considering the participation of the well-known paramagnetic defect centers of the E′, NBOHC and POR. Such new variants of the O_2^--type defect centers as observed in neutron irradiated specimens were not observed. The production of these states might be difficult to observe in the present case of rather high dpa values as discussed below.

In the resolution of each spectrum, the initial g-values and peak-to-peak derivative widths of Lorentzian line shapes for the E′, NBOHC and POR were taken from our previous study [3]. A line shape simulation was performed similar to the case in the literatures [4–6], and a least squares fitting method was applied to the simulation in order to determine the g-values and peak-to-peak derivative widths of the component defects. The results are summarized in Table 1.

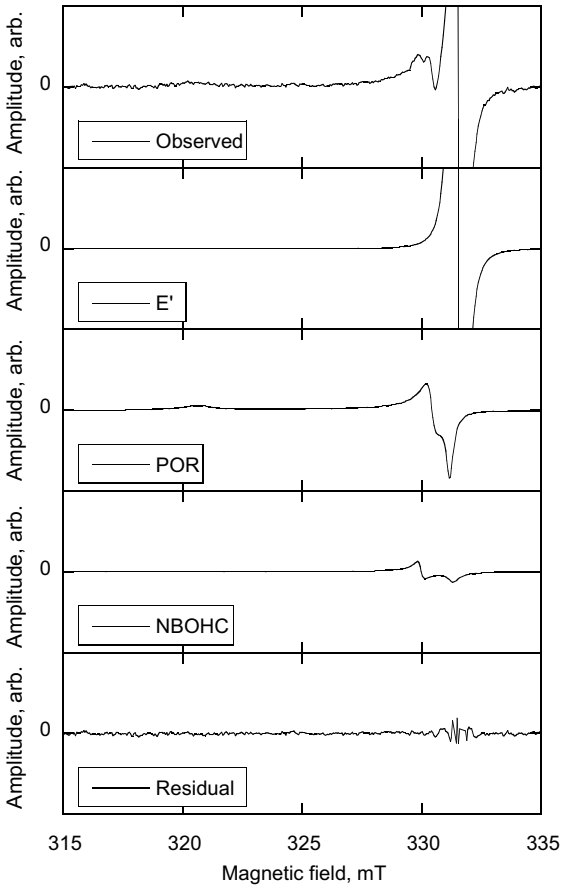

Fig. 1. Typical X-band ESR spectrum of the 2 MeV He$^+$ irradiated vitreous silica (T-2030) and its components: (a) observed spectrum (2.0×10^{18} ions m^{-2}), (b) E′, (c) POR, (d) NBOHC, (e) others.

Contrary to the present study using 2 MeV He$^+$ ions, Miyamaru et al. [7] have observed the ESR signal of $g = 2.0025$ is much higher than that of the E′ in their study using 20 keV D$^+$ and He$^+$ ions. By considering different incident energies, it may be postulated that they have observed the defect species produced near surface. According to Stesmans and Scheerlinck [8], in fact, the

Table 1
g-Values and peak-to-peak derivative widths determined in the present analysis

Defects	g-Value			Peak-to-peak derivative width		
	g_1	g_2	g_3	σ_1	σ_2	σ_3
E′	2.0003	2.0005	2.0017	0.05	0.05	0.05
POR	2.002	2.007	2.067	0.1	0.2	1
NBOHC	2.001	2.010	2.08	0.1	0.3	3

so called EX centers with $g = 2.0025$ are produced around surface.

3.2. Effect of ion beam intensity and fluence

Fig. 2 shows the ion beam intensity dependence of the spin densities of the E′s, NBOHCs, and PORs. Although the intensity ranges from 4.5×10^{-4} to 4.5×10^{-3} A/m^2, no apparent effect is observed on each spin density. As shown below, a cascade overlap effect is inferred from the ion beam fluence dependence, but there is almost no effect of the ion beam intensity in the studied range.

Fig. 3 shows the effects of ion beam fluence on the spin densities of the E′s, NBOHCs, and PORs. For comparison, the results of neutron irradiation are also shown in the figure as a function of the dpa value. A conversion factor of 1 dpa $= 1.8\times10^{24}$ n/m^2 for oxygen is obtained for fast neutrons following the manner in the literature [9,10], while the dpa values of ion beam irradiation are evaluated by using the TRIM code (SRIM-98). In the latter case, by considering inhomogeneous defect production and by taking a weighted average value for dpa, a conversion factor of 4.4×10^{20} ions/m^2 for oxygen is obtained for 2 MeV He^+ ions. In Fig. 3, it is seen that the dpa values of the present ion beam irradiation are much higher than those of neutron irradiation [3]. In such a case, the contribution of the impurity (OH) related defect centers may be negligible. This is the reason why such variants of the O_2^--type defect centers as observed in neutron irradiated specimens are not observed in the present case.

As shown in Fig. 3, the spin densities of the E′s, NBOHCs, and PORs increase with the increasing dpa value. Above the dpa value of 10^{-2}, however, all the spin densities become saturated. Cascade overlaps are considered to be responsible for this saturation behavior, and defect clusters are produced in this region. As for the production efficiency of the defect centers, it is noted that the spin densities of the E′s are rather close to the evaluated concentration of the displaced oxygen atoms, especially in the case of ion beam irradiation. This means the production efficiency of the E′s is considerably high. Not only the nuclear stopping but also the electronic stopping power may be considered to take part in such a high production efficiency in this case.

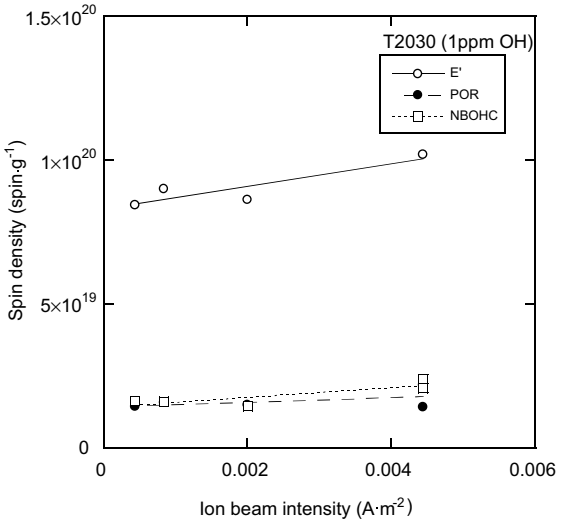

Fig. 2. Ion beam intensity dependence of spin densities in the 2 MeV He^+ irradiated vitreous silica (T-2030). Dose: 1.5×10^{19} ions m^{-2}.

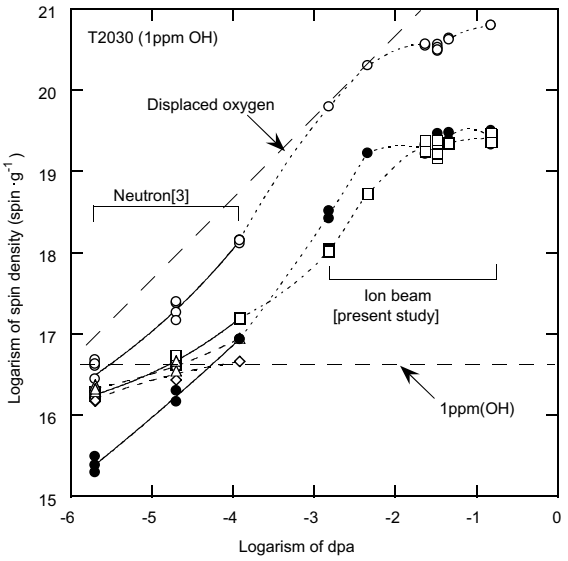

Fig. 3. Dpa dependence of spin densities in the 2 MeV He^+ irradiated and neutron irradiated vitreous silica (T-2030). Results of neutron irradiation are from the literature [3]. ○: E′, ●: POR, □: NBOHC, △ and ◇: variants of the O_2^--type defect centers. Curves are drawn for aid of the eyes.

Among the other defects, it may be remembered that diamagnetic oxygen-deficiency centers such as ODCs are also produced in vitreous silica. In fact, the production of the ODCs has been observed by an in situ luminescence measurement of vitreous silica in our previous study [11]. It is thus interesting to compare the production efficiencies of all these defects, and a comparison will be given below.

3.3. Production and reaction mechanism

In our previous study on neutron irradiated vitreous silica [3], a production and reaction mechanism has been used to explain the obtained results. The same mechanism is applied here to the present results.

The production of the E′s under irradiation may be expressed as

$$(\equiv \mathrm{Si{-}O{-}Si} \equiv)^* \rightarrow \equiv \mathrm{Si^{\cdot}Si} \equiv + \mathrm{O}^- \quad (1)$$

where $(\equiv \mathrm{Si{-}O{-}Si} \equiv)^*$ denotes an excited state produced by irradiation. Also, the PORs are produced from the E′s and O_2 molecules by [12]

$$\equiv \mathrm{Si^{\cdot}Si} \equiv + \mathrm{O_2} \rightarrow \equiv \mathrm{Si{-}O{-}O^{\cdot}Si} \equiv \quad (2)$$

Because of rather high activation energy ($E = 1.17$ eV [13]) for the O_2 diffusion, however, Griscom and Mizuguchi [2] pointed out that reaction (2) hardly occurs at lower temperatures. By considering possible break up of the O_2 molecules by neutron irradiation [14], they suggested the following reactions for the production of the NBOHCs and PORs at lower temperatures.

$$\equiv \mathrm{Si^{\cdot}Si} \equiv + \mathrm{O}^0 \rightarrow \equiv \mathrm{Si{-}O^{\cdot}Si} \equiv \quad (3)$$

$$\equiv \mathrm{Si{-}O^{\cdot}Si} \equiv + \mathrm{O}^0 \rightarrow \equiv \mathrm{Si{-}O{-}O^{\cdot}Si} \equiv \quad (4)$$

The O^0s are also produced by irradiation together with the diamagnetic ODCs [11] as

$$(\equiv \mathrm{Si{-}O{-}Si} \equiv)^* \rightarrow \equiv \mathrm{Si : Si} \equiv + \mathrm{O}^0. \quad (5)$$

Although some variants of the O_2^--type defect centers (X_1s and X_2s [11]) are also involved in the mechanisms at lower dpa values, the observed dpa dependence of the spin densities of the E′s, NBOHCs, and PORs in Fig. 3 are well explained by considering these reactions.

3.4. Isochronal anneal behavior of spin densities

Fig. 4 shows the results of the isochronal anneal of vitreous silica (T-2030) irradiated by 2 MeV He^+ ions to a dose of 1.5×10^{19} ions/m^2. The observed annealing behavior is well explained by considering the above reactions. For example, the spin densities of the E′s rapidly decrease with the increasing temperature up to 473 K (200 °C) possibly due to their recombination with the O^-s which are adjacent to the E′s. The recombination is not completed below 473 K, but the remaining E′s may recombine with the O^-s which are apart from the E′s, at high temperatures at which such O^-s are expected to be mobile.

As for the others, it may be noted that the NBOHCs decreases and the PORs to increase with the increasing temperature in a rather lower temperature region. As pointed out by Griscom and Mizuguchi [2], reactions (3) and (4) are considered to be responsible for this behavior, since reaction (2) hardly occurs at lower temperatures. No apparent increase of the PORs is observed at higher temperatures above 573 K (300 °C), and almost no contribution of reaction (2) is inferred from the present results.

As mentioned above, it is interesting to evaluate the densities of such diamagnetic ODCs from the present

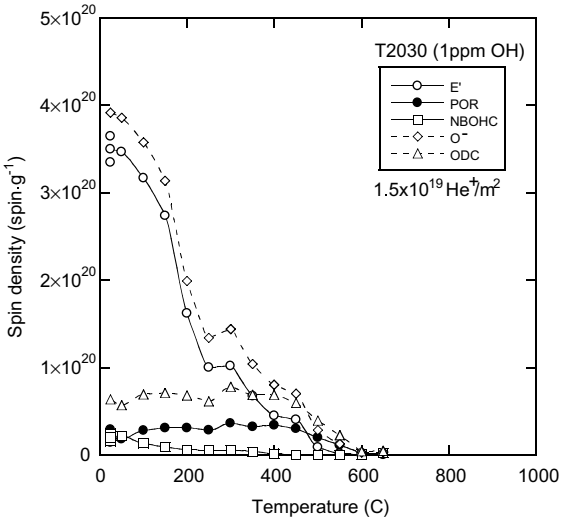

Fig. 4. Ten-minute isochronal anneal experiment of the 2 MeV He^+ irradiated vitreous silica (T-2030). Dose: 1.5×10^{19} ions m^{-2}.

results. For the O^0s which are produced together with the ODCs by reaction (5), it may be assumed that its density will be relatively small because of its high mobility. By considering the above reaction scheme and mass balance, the densities of the ODCs and O^-s are thus given by

$$N_{\mathrm{ODC}} = N_{\mathrm{NBOHC}} + 2N_{\mathrm{POR}}, \quad (6)$$

$$N_{\mathrm{O^-}} = N_{\mathrm{E'}} + N_{\mathrm{NBOHC}} + N_{\mathrm{POR}}, \quad (7)$$

where N denotes the density. Together with the ODCs, the O^0s are produced by reaction (5) and are used to produce the NBOHCs and the PORs by reactions (3) and (4). Then Eq. (6) is obtained by considering that one NBOHC corresponds to one O^0 and one POR to two O^0s. Eq. (7) is also obtained similarly by considering reactions (1), (3) and (4).

The densities of the ODCs and O^-s are evaluated from the present results by using Eqs. (6) and (7), as shown in Fig. 4. It is natural that the density of the O^-s is almost the same as those of the E′s. As for the ODCs, it is recognized that the density of the ODCs is much lower than that of the E′s. The production efficiency of the ODCs is not so high as that of the E′s in vitreous silica.

4. Conclusions

In order to know the production behavior of irradiation defects in vitreous silica, ESR measurements were performed in the present study. The spin densities of the

E′s, NBOHCs, and PORs were measured in the ion beam irradiated specimens and compared with the results of neutron irradiation. Both results were well explained by considering the dpa values of irradiation. It was found that the production efficiency of the E′s is considerably high.

Based on the proposed production and reaction mechanism, the densities of such diamagnetic ODCs were also evaluated from the present results. It was found that the production efficiency of the ODCs is not so high as that of the E′s.

References

[1] L. Skuja, J. Non-Cryst. Solids 239 (1998) 16.
[2] D.L. Griscom, M. Mizuguchi, J. Non-Cryst. Solids 239 (1998) 66.
[3] K. Moritani, I. Takagi, H. Moriyama, J. Nucl. Mater. 325 (2004) 169.
[4] R.A.B. Devine, Phys. Rev. 35 (1987) 9783.
[5] D.L. Griscom, J. Non-Cryst. Solids 149 (1992) 137.
[6] T. Tabata, M. Hasegawa, M. Fujinami, Y. Ito, H. Sunaga, S. Okada, S. Yamaguchi, J. Nucl. Mater. 239 (1996) 228.
[7] H. Miyamaru, T. Tanabe, T. Iida, A. Takahashi, Nucl. Instrum. and Meth. B 116 (1996) 393.
[8] A. Stesmans, F. Scheerlinck, J. Appl. Phys. 76 (1994) 1047.
[9] M. Hasegawa, M. Saneyasu, M. Tabata, Z. Tang, Y. Nagai, T. Chiba, Y. Ito, Nucl. Instrum. and Meth. B 166&167 (2000) 431.
[10] C.H. de Novion, A. Barbu, Solid State Phenom. 30&31 (1993) 277.
[11] K. Moritani, I. Takagi, H. Moriyama, J. Nucl. Mater. 312 (2003) 97.
[12] A.H. Edwards, W.B. Fowler, Phys. Rev. B 26 (1982) 6649.
[13] F.J. Norton, Nature 191 (1961) 701.
[14] L. Skuja, B. Güttler, Phys. Rev. Lett. 77 (1997) 2093.